ELSEVIER

Vibrational Spectroscopy 25 (2001) 119–131

VIBRATIONAL SPECTROSCOPY

www.elsevier.com/locate/vibspec

Mode assignment for linear phenyl acetylene sequence: phenylacetylene, di-phenylacetylene and 1,4-di(phenylethynyl)benzene

Z. Chernia*, T. Livneh, I. Pri-Bar, J.E. Koresh

Nuclear Research Center Negev, P.O. Box 9001, Beer Sheva 84190, Israel

Received 5 September 2000; accepted 7 November 2000

Abstract

Normal mode derivation for a large molecule at the harmonic approximation level, is still, a demanding task for ab initio large-size basis or functional densities methods. Build in-process additive errors, affect the accuracy and often limit the applicability of such.

It is argued here, that in cases, where point group symmetry of a large molecule is not lower then the symmetry of the related structural ''building-block'', normal mode unfolding scheme could be effectively predicted from group theory considerations and the vibrational structure of the building block. A simple semiempirical Hamiltonian could be then utilized in order to obtain a mode assignment for the large molecule. In the present study, vibrational mode assignment for members of a poly-phenylacetylene linear chain: 1,4-di(phenylethynyl) benzene (DPB), diphenylacetylene (DPA) and phenyl acetylene (PA) is obtained. Their structure was calculated by means of the computationally efficient semiemprical RHF PM3 Hamiltonian. Raman and FTIR spectra were taken and assign with mutual correspondence for the three compounds. The remaining weak peaks observed in the spectra were successfully described as overtones and combinations. Few medium sized modes were identified as Fermi resonances. The overall, mode-unfolding scheme of the DPB, which was originated in the DPA, which in turn was originated in the PA, was established. The successive elements of the linear poly-phenylacetylene chain are all members of a same D_{2h} point group, except the phenyl acetylene which is of lower C_{2v} point group. It is argued here, that the same principle allows us to predict the unfolding scheme further for linear DPB . . . + PA, but not for the lower symmetry phenyl acetylene macro cycles.

Keywords: 1,4-Di(phenylethynyl)benzene; Diphenylacetylene; Phenyl acetylene; PM3; Overtones; Combinations; Fermi resonance; D_{2h}; C_{2v}

1. Introduction

1,4-Di(phenylethynyl)benzene (DPB), diphenylacetylene (DPA) and phenyl acetylene (PA) are three basic building blocks for a group of linear phenyl acetylene sequence (LPAS) and phenyl acetylene macro cycles (PAMC) [1,2]. These macromolecules crystals have remarkable stability and high melting points, which were attributed to effect of binding which originated from ''π-stacking interactions'' [3]. The unusual ''π–π interactions'' of such stacks can explain some metal catalyzed reactions of solid DPA and DPB [4]. Recently, a self assembled monolayer of oligo(phenylethynyl) benzenethiol was synthesized, displaying a dense packed structure with a highly ordered pattern [5].

* Corresponding author.
E-mail address: c_zelig@bezeqint.net.il (Z. Chernia).

0924-2031/01/$ – see front matter
PII: S0924-2031(00)00114-4

The molecular structure of elements such as DPA and PA, was examined by advanced semiempirical and ab initio methods in the past. Their vibrational structure was calculated and corrected by the standard scaling algorithms in order to fit the observed IR and Raman vibration spectra [6–8]. Their planar structure was assigned to the point groups symmetry of D_{2h} and C_{2v}, respectively. However, ab-initio or density functional calculations are effectively limited by the complexity of the molecule. The complexity of computation can be significantly reduced, by applying symmetry arguments extracted from collective group analysis. Therefore, an alternative approach should be examined, for which the vibrational structure of D_{2h} symmetry LPAS is rigorously described in terms of the vibrational structure analysis of their DPA and PA building blocks. Here, semiempirical SCF-HF algorithm is employed for this approach, while utilizing DPB as the test case for the study.

Scaling procedures were developed by Meyer and Pulay [9], Botschwina [10,11] and Blom and Altona [12–15] in order to fit the calculated and the experimental normal mode frequencies, measured by the Raman and FTIR techniques. Normally, a Born–Oppenheimer (B–O) harmonic approximation was applied at a top of a charge distributed, geometry optimized structure. Relatively large deviations of tenths or hundreds of wavenumbers in calculated mode vibrations were found for many compounds [16]. The observed discrepancies were due to the limitation of the B–O harmonic approximation, as well as to difficulties in assigning the correct distributed charge and optimizing the exact geometry at equilibrium. Scaling procedures usually artificially optimizes the force-constants set of internal coordinates of the parent molecules, which are then applied to the examined molecule. It is a tedious procedure, which depends entirely on a priori intuitive assignment of the experimental data. It was helpful in the reported works where showed accurate results [17]. However, it is essentially a pure mathematical optimization routine, binding together various errors of a possible different physical origin and in some cases may be avoided.

The purpose of this study is to examine the possibility of deducing vibrational structure of a molecule from the vibrational assignment of its building blocks. This scheme requires that the symmetry of a more complex system is not lower than the symmetry of its constituents. It is pointed out, that only few systems would meet those restrictions and that such a system should be represented by a similar to its precursor's internal coordinates set.

Structurally, DPB may be viewed as co-axially welded, partially overlapping pair of DPAs. Both molecules obey the D_{2h} point-symmetry restrictions. Due to the dominance of the skeletal forces, which are practically similar in the two molecules, no corrections for the original DPA force constants are needed in order to calculate the DPB normal modes. Hence, the geometry of a relevant pair of the DPA normal modes is sufficient to approximate the geometry of the resultant DPB proper mode (only when the group symmetry requirements are fully complied). It is also argued in this work that DPA own mode symmetry correspondence, originated from a pair of the phenylacetylene-like species. Here, our goal was to analyze DPB normal mode symmetry, by examining vibrations originated in the DPA, then to look for a possible DPAs core-structure. Hence, normal mode assignment is obtained in correspondence to the measured spectra taken by FTIR and Raman complementary techniques for DPB–DPA–PA sequence. This is accomplished by a three steps scheme: (a) establishing the correspondence between the DPA and DPB (PA and DPA) normal modes and classifying the derived modes in four common subgroups, according to their symmetry features; (b) further classifying modes in each subgroup according to their origin; (c) identifying each calculated normal modes subgroup (for the complete sequence: PA, DPA and DPB in correspondence), in the FTIR and Raman vibrational spectra.

2. Experimental

PA obtained from Aldrich at 98% purity, was used after distillation under vacuum. DPA was purchased from Aldrich at 98% purity. DPB was synthesized by a palladium catalyzed coupling of PA derivatives with the appropriate mono- or di-bromobenzene [18]. Coupling products were purified by re-crystallization and analyzed by NMR.

FTIR spectra were recorded at 2 cm^{-1} resolution, on a Nicolet Magna 550 purged spectrophotometer, equipped with KBR optics and DTGS detector. The

spectrum of a pure liquid phenylacetylene sample was taken by transmission. Small internal refraction ''ripples'' caused by the use of a thin 25 μm spacer in the transmission cell accessory, could not be totally eliminated by the empty cell referencing. The DPB and the DPA samples were prepared by dissolving the compounds in chloroform, then evaporating the sub-saturated mixture on the KBR powder. The IR spectra were taken by diffuse reflectance.

The Raman spectra were measured in a back-scattered configuration with a Renishaw micro-Raman spectrometer, using a He–Ne laser (632.8 nm) as a source. The spectral resolution provided by the holographic grating (1800 grooves per millimeter) was better than 2 cm^{-1}. The same as in IR measurement phenylacetylene sample was used. The DPB and the DPA samples were prepared by evaporating the dissolved in chloroform compounds upon 1 mm thick Si wafer. All the spectra were baseline corrected.

3. Computational details

Semi-empirical methods are generally considered inferior to the modern ab initio or FD based calculations. However, semiempirical derivations of the molecular geometry by the AM1 and PM3, are comparable in accuracy to those obtained by using medium size basis ab initio calculations. Vibrational frequencies derived from these methods are comparable in accuracy to large basis set ab initio calculations [12,16]. For the basic vibrational analysis, no elaborated electron-correlation energy corrections at the CI level are required. Moreover, the integral-overlapping parameter-sets for the semi-empirical methods are best optimized for hydrocarbons. Hence, semi-empirical methods are particularly suited for the present case.

All the semiempirical calculations were performed on a MOPACs computational package implemented in HyperChem 5.0 software. The computational procedure included geometry optimization at a Restricted Hartree–Fock level PM3 algorithm. The optimization process was set at several different starting non-planar positions, without any a priori constraint on the molecular structure. In all cases, a planar D_{2h} geometry was achieved. The vibrational analysis was performed with a standard B–O harmonic approximation. The normal mode motions were derived, and the symmetry representations were then established. From the two spectroscopic techniques utilized, only the IR active mode intensities could be calculated in the software.

We note that starting at a non-symmetry-confined geometry, vibrational calculation lead, in few cases to some minor distortions in the derived modes, making the assignment difficult. However, thorough examination reviled the correct symmetry type. Consequently, these distortions resulted in minor changes in the calculated IR intensities and in some cases, to the assignments of low absorption coefficients to the IR-inactive vibrations (which were naturally disregarded).

4. Discussion and results

4.1. Geometry optimization

The widely used AM1 and PM3 self consistent field methods are based on a same mathematical derivation. They differ only in the values of their overlapping integral parameters [19,20]. In this study (as in some other reports [21]), the AM1 based geometry was outperformed by the more recent PM3 parameter-set. Table 1 shows the derived geometry in PM3 according to the definitions of Fig. 1, along with the reported results of the ab initio 4-31G calculations and the XRD measurements [6,7]. The calculated C–C bond distances in general are slightly overestimated by all RHF SCF methods. Here, for both compounds: DPA and DPB, distances and angles at analog positions were calculated to be similar and in fairly good agreement with the experimental data.

4.2. Group theory considerations

The normal mode symmetry assignment was obtained from observing the animated molecule vibrations. Since the both DPB and DPA point symmetry are D_{2h}, the mode scheme of DPB may expected to be constructed from different in-phase or out-of-phase super-positions of a pair of a parent DPA molecules, welded together as shown in Fig. 2. The D_{2h} point symmetry is fully describable by eight mode (A_g, B_{1g}, B_{2g}, B_{3g}, B_{1u}, B_{2u}, B_{3u}, A_u) irreducible representation, defined under the point symmetry operations. Only at

Table 1
Calculated geometry of PA, DPA and DPB

Bond Type	PA by XRD	DPA by XRD	DPA by 4-31G	DPB or DPA (PA) by PM3[a]
C1–C8	1.208	1.198	1.194	1.195 (−0.003)
C1–C2	1.448	1.438	1.431	1.415 (+0.003)
C5–C6	1.398	1.367	1.384	1.391 (0.0)
C6–C7	1.396	1.376	1.381	1.390 (0.0)
C2–C7	1.388	1.383	1.392	1.399 (0.0)
C8–C1–C2	NA	178.3	NA	179.9 (0.0)
C1–C2–C3	NA	120.0	NA	120.0 (0.0)
C4–C5–C6	119.9	120.1	119.8	120.1 (0.0)
C5–C6–C7	119.9	120.3	120.2	120.2 (0.0)
C6–C7–C2	119.8	120.1	120.4	119.7 (0.0)
C7–C2–C3	120.8	119.1	119.0	120.1 (0.0)

[a] Calculated geometry in this work; deviations for the PA in parentheses.

a full compliance to one of the eight mode representations, a proper DPB mode-composition (derived from a pair of the parent DPA modes) is symmetry-allowed.

Fig. 3 demonstrates DPB-normal mode unfolding scheme for #86, #85 and #84 and DPA #55 and #54, which are ring-stretching vibrations (the mode index format is defined according to the ascending energy-level criterion). The DPB modes are composed of one of the parent #55 or #54 DPA mode's pair, each. A pair of #55 B_{1u} modes constructs the #86 A_g and #85 B_{1u} modes, while a pair of #54 A_g modes, shapes the #84 A_g.

Different evolution scheme is applied when the two modes are almost degenerate energetically, as for DPB ring-deformation stretching modes: #83, #81. These modes evolve from the #53, #52 DPA pairs, as shown

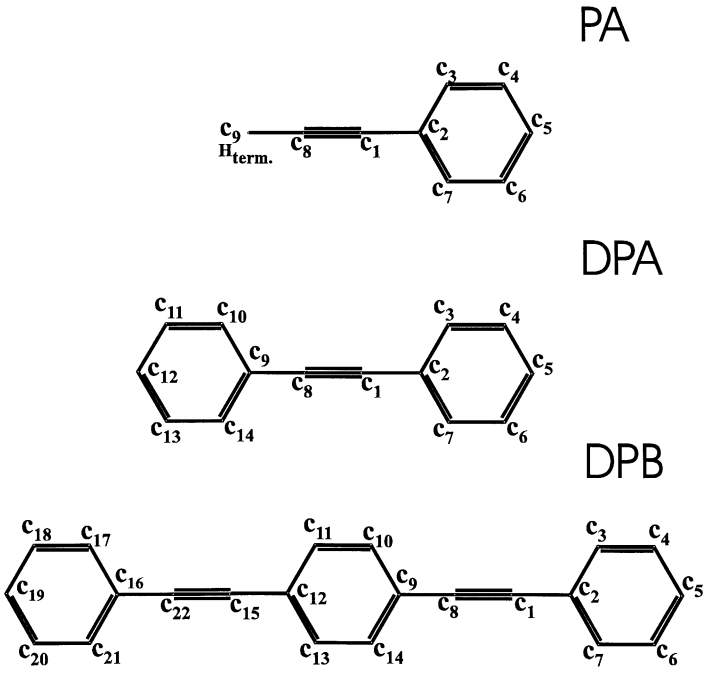

Fig. 1. Numbering scheme in PA, DPA and DPB.

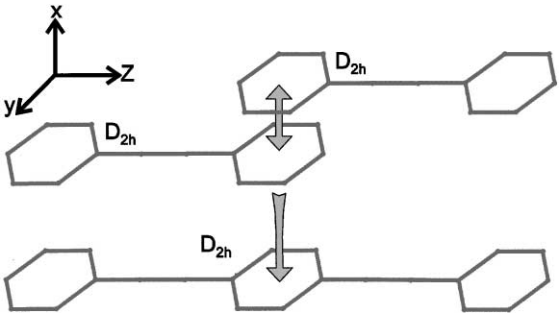

Fig. 2. DPB mode formation scheme by DPA mode overlapping.

in Fig. 4. First, each parent normal-mode ''gave birth'' to it's own clone (#52 $B_{3g} \rightarrow$ #83 B_{3g} and #53 $B_{2u} \rightarrow$ #82 B_{2u}). The exact, mirror-like symmetric (anti-symmetric) nature of the degenerate #53, #52 pairs, implies that each DPA mode may be viewed as if it has been assembled by a pair of in-phase (out-of-phase) non-interacting precursor mode components (related to the PA-like modes geometry). Consequently, these degenerate DPAs mode pairs (#53 $\times$ 2, #52 $\times$ 2), dictates the degenerate character of the resultant #83, #82 DPB modes. However, the #81 B_{3g} can not be assigned to a direct product of any of its parents solely, but rather to a virtual $B_{3g} \pm B_{2u}$ mode which is a direct sum of the #53+ #52 mode pair.

For a non-degenerate DPB modes (#86, #85 and #84), which in some cases are split by tenths of wavenumbers, the interaction energy within the mode constituents, is obviously large enough to enable the distortion of the perfect in-phase (out-of-phase) mode geometry. Consequently, the origin of the followed DPB modes is difficult to relate to.

Figs. 3 and 4 demonstrate a common evolution pattern according to which, the outcome of the B_{3g}, B_{2u}, A_g and B_{1u} DPA mode representations will always remain the same in the representation of the DPB modes. This symmetry-conservation feature can be applied for the four others mode representations as well. Hence, we call A_g and B_{1u} a sub-group ''A'' and B_{2u} and B_{3g} a subgroup ''B'' of the D_{2h} symmetry group. In a similar way the A_u with the B_{1g} and B_{3u} with the B_{2g} will compose the sub-groups ''C'' and ''D'', respectively (see Table 2). Therefore, in practice, the aforementioned symmetry compliance condition can be effectively confined to examination of only two mode irreducible representations, which are the only feasible types for each composed normal mode of the DPB. The four members of the ''A'' and

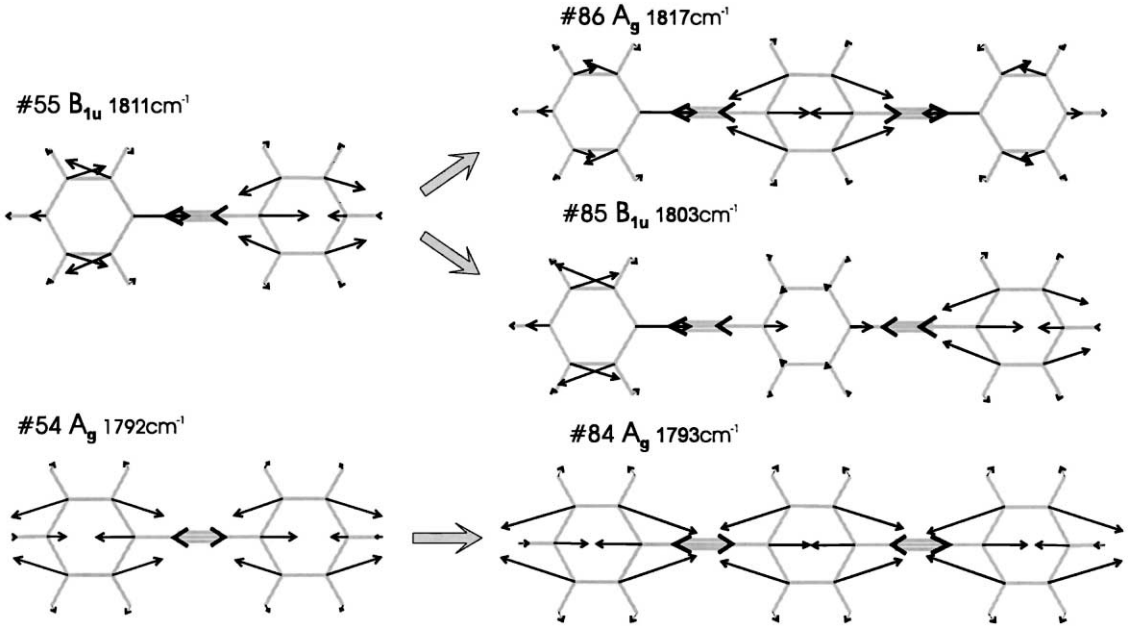

Fig. 3. Representative evolution-scheme of an interacting (along the acetylene C≡C bond) DPAs C–Ph stretching mode pair (#54 and #55), into the respective DPBs threefold mode pattern (#84, #85 and #86).

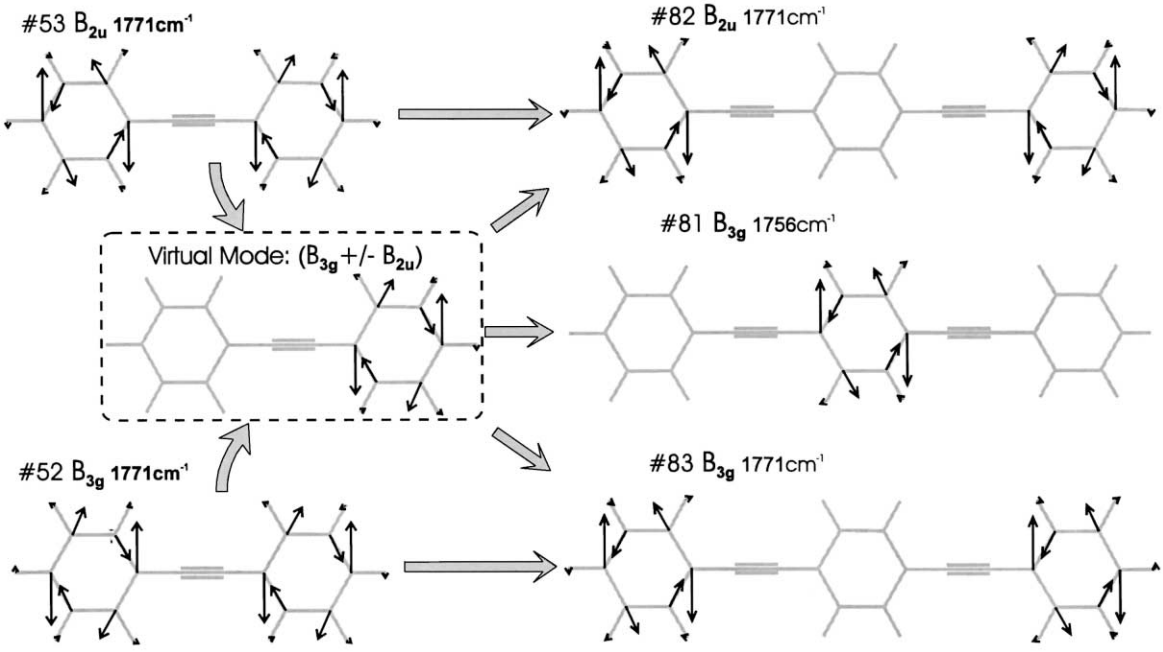

Fig. 4. Representative evolution-scheme of a non-interacting DPAs phenyl-deformation mode pair (#52 and #53), into the respective DPBs threefold mode pattern (#81, #82 and #83).

''B'' subgroups are in-plane types, the members of the ''C'' and ''D'' subgroups, vibrates out-of-plane. A question arises: what is the origin of this four-subgroup partitioning scheme? In order to answer this question, we have to examine the DPA symmetry precursor.

DPA core-specie is represented by PA molecule of C_{2v} point group symmetry. The calculated in-phase

Table 2
Mode representations for DPA and DPB[a]

Symmetry Types D_{2h}	Subgroup	DPA	DPB	Optical Activity	Symmetry Types C_{2v}[b]
A_g	A	12	18	Raman	A_1
B_{1u}	A	11	17	IR	
B_{2u}	B	11	17	IR	B_2
B_{3g}	B	11	17	Raman	
A_u	C	4	6	Inactive	A_2
B_{1g}	C	3	5	Raman	
B_{2g}	D	7	11	Raman	B_1
B_{3u}	D	7	11	IR	
		Total=66	Total=102		

[a] Mode counting derived from group theory predictions, based on D_{2h} geometry of Fig. 1.

[b] The evolution of the C_{2v} point group types to modes of D_{2h} point group symmetry is in compliance with group theory predictions according to [22].

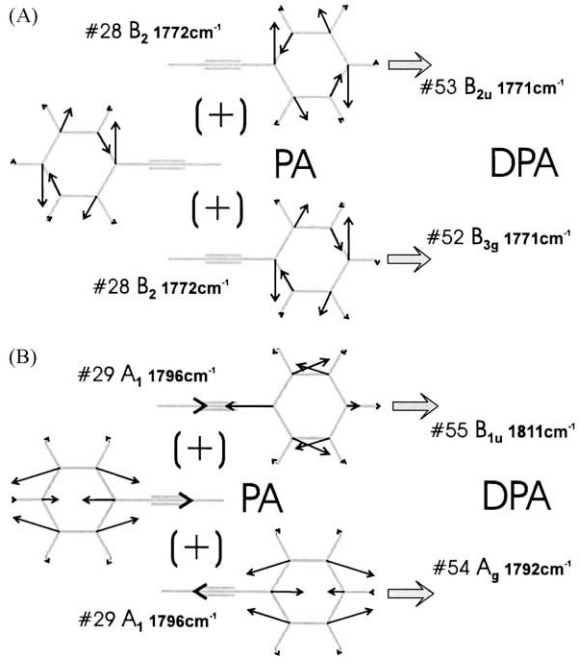

Fig. 5. Evolution of the PA non-interacting: (A) #28; and the interacting (along the acetylene C≡C bond): (B) #29 modes, into the respective DPAs twofold mode pattern (#52, #53 and #54, #55).

(out-of-phase) normal modes resulted combinations, accurately reproduces the DPA modes. Fig. 5 demonstrates evolution of DPA #52÷#55 normal modes from their respective PA precursors. Consequently, a pair of PA #28 B_2 mode combinations evolved into DPA #53 B_{2u} and #52 B_{3g} normal modes and into subsequent DPB #83 B_{3g}, #82 B_{2u} and #81 B_{2u}. A pair of PA #29 A_1 combinations evolved into DPA #55 B_{1u} and #54 A_g modes, then into following DPB #86 A_g, #85 B_{1u} and #84 A_g. This unfolding scheme is in full compliance with the group theory predictions, for the evolution of the C_{2v} point group specie to a higher D_{2h} symmetry molecule. A full $D_{2h} \leftarrow C_{2v}$ transformation is presented in the last column of Table 2.

To summarize, the four ''A'', ''B'', ''C'', ''D'' subgroups of the DPB (DPA) previously postulated, are merely the four irreducible representations of the phenyl acetylene like C_{2v} specie.

4.3. Mode assignment

There are a total of 66 and 102 normal vibrational modes for the DPA and DPB, respectively. Due to the inversion symmetry, a mutual exclusion rule restricts the optical activity of the normal modes to be observed either in IR or in Raman (Table 2). Here, A_g, B_{1g}, B_{2g}, B_{3g} are Raman active, B_{1u}, B_{2u}, B_{3u} are IR active and A_u is optically inactive. According to group theory predictions for the DPB (DPA) molecule, 45 (29) normal modes are IR active, 51 (33) normal modes are Raman active and six (4) are optically inactive. All of the C_{2v} symmetry types of the PA are Raman and IR active, accept the A_2 symmetry representation, which is IR forbidden.

Following the rules mentioned above, mode assignment could now be conducted. First, PA, DPA and DPB vibrational spectra were acquired by Raman and FTIR. In each molecule, normal modes were analyzed and assigned in accord with their respective sub-group member, a spectrum of which is taken by the complementary technique (Raman or FTIR). Then, DPA and DPB were analyzed, while the mutual modes correspondence is taken as a governing rule. In many cases, it was necessary to examine further the correlation of the DPA-DPB modes by cross checking their position with those of PAs. Table 3 summarizes the assignment of all the modes and compares the observed versus calculated normal frequencies, with the symmetry and sub-group attribution specified for each mode.

Since spectra of more then a hundred normal modes in several compounds, taken by different spectroscopic techniques and experimental conditions are assigned, few undoubted spectral assignments of the most intense bands (IR with a corresponding Raman), served as ''anchoring points'' to ease locating the nearby, less intense modes. These are the normal modes of the subgroups: A8, A7, B8, D6, D5, D4 and D3, covering the: $500 \div 1800\ cm^{-1}$ spectral region.

D3 subgroup modes are out-of-plane C–Ph bending vibrations. Some of the calculated mode frequencies are higher by up to 8% then the experimental values. All of the subgroup members are well correlated with each other according to the classic unfolding scheme and are easily recognized in Raman and FTIR spectra. PA B_1 mode found at 513 cm^{-1} in IR and at 522 cm^{-1} in Raman, was split in DPA in 509 cm^{-1} IR absorption mode and 543 cm^{-1} Raman. Each branch was further split in DPB molecule in 470 cm^{-1} (Raman), 523 cm^{-1} (IR) and 537 cm^{-1} (Raman), 550 cm^{-1} (IR),

Table 3
Normal mode assignment and description for DPB, DPA and PA[a]

DPB Mode #	Sub-Group	DPB Mode Type	DPB ν[cm^{-1}] (calc.)	DPB ν[cm^{-1}] (meas.)	DPA Mode #	DPA Mode Type	DPA ν[cm^{-1}] (calc.)	DPA ν[cm^{-1}] (meas.)	PA Mode #	PA Mode Type	PA ν[cm^{-1}] (calc.)	PA ν[cm^{-1}] (meas.) IR ; Raman	Mode Description ***
1	C1	A_u	-8	NA	1	A_u	35	NA	-				Ph ž-twist
2	C1	B_{1g}	8	NA	1				-				
3	D1	B_{3u}	18vw	NA	3	B_{3u}	52 w	NA	1	B_1	137 m	NA ; NA	Ph ⊥bend
4	B1	B_{2u}	22vw	NA	2	B_{2u}	51 w	NA	2	B_2	176 m	NA ; NA	C-Ph ∥ bend
5	B1	B_{3g}	53	NA	2				2				
6	D1	B_{2g}	56	NA	3				1				
7	D1	B_{3u}	100 w	NA	4	B_{2g}	135	147vw	1				
8	B1	B_{2u}	141vw	NA	5	B_{3g}	172	174vw	2				
9	D1	B_{2g}	164	~182w	4				1				
10	A1	A_g	184	~182w	7	A_g	283	261 s	5	A_1	491vw	465vw;473vs	Ph ž-def.
11	B1	B_{3g}	196	~182w	5				2				
12	D2	B_{3u}	245 m	NA	6	B_{3u}	264 w	* 280 s	3	B_1	350 s	349s; 361vs	C-Ph ⊥bend
13	D2	B_{2g}	320	334 m	6				3				(boat)
14	C2	A_u	356	NA	8;9	B_{1g} ;A_u	358;	407w;	4	A_2	358	NA; 407vw	
15	C2	B_{1g}	356	402vw	8;9		…358	…NA	4				Ph ⊥def.
16	C2	A_u	356	NA	8;9				4				
17	A1	B_{1u}	358vw	NA	7				5				
18	D2	B_{3u}	400vw	NA	10	B_{2g}	395	388 s	3				
19	B2	B_{2u}	462 s	450 s	11	B_{2u}	482 m	467 m	7	B_2	565 s	530s; 535s	C-C≡C ∥-bend
20	D3	B_{2g}	465	~ 470m	12	B_{3u}	503 s	509vs	6	B_1	537vw	513m; 522sh	
21	B2	B_{3g}	501	~ 477m	11				7				
22	D3	B_{3u}	525vs	523vs	12				6				
23	A1	A_g	537	554 w	13	B_{1u}	556 w	536 s	5				
24	D3	B_{2g}	576	537 m	14	B_{2g}	585	543 s	6				C-Ph ⊥bend
25	D3	B_{3u}	612vs	550 s	14				6				(chair-boat)
26	B3	B_{3g}	622	630 w	15	B_{3g}	621	626 s	8	B_2	628 w	~622; ~624	
27	B3	B_{2u}	624vw	623 w	15;16	B_{3g};B_{2u}			8				Ph ∥-def.
28	B3	B_{3g}	633	654 w	16	B_{2u}	628vw	620 w	8				
29	D4	B_{2g}	656	691vw	17	B_{3u}	650vs	690vs	9	B_1	656vs	690vs; NA	C-Ph ⊥bend
30	D4	B_{3u}	662vs	692vs	18	B_{2g}	669	710 s	9				(chair)
31	A2	B_{1u}	669 m	667 m	20	A_g	754	691 m	11	A_1	836 w	843w; 848w	Ph ž-def.
32	B2	B_{2u}	671vw	~667	19	B_{3g}	680	658vw	7				
33	B2	B_{3g}	696	662sh	19				7				
34	D5	B_{2g}	713	727 m	21;22	B_{3u}; B_{2g}	779vs;	756vs;	10	B_1	781vs	762vs; 768vs	
35	D5	B_{3u}	783vs	754vs	21;22		…788	…760 s	10				C-H ⊥bend
36	D5	B_{2g}	783	761 w	21;22				10				
37	A2	A_g	789	776vw	20				11				
38	C3	B_{1g}	845	810vw	23;24	A_u; B_{1g}	847;	NA;	12	A_2	848	NA; 850 vw	C-H ⊥bend…
39	C3	A_u	847	NA	23;24		…847	…833w	12				+ Ph ž-twist
40	C3	B_{1g}	847	832vw	23;24				12				

Table 3 (*Continued*)

41	**A2**	B_{1u}	885 vw	848 sh	25	B_{1u}	906 vw	851 w	11				
42	**D6**	B_{3u}	886 vs	839 vs	26;27	B_{3u}; B_{2g}	941 vs;	918 vs;	15	B_1	943 s	918 s; 928 vw	**C-H ⊥bend… Ph -boat bend**
43	**D6**	B_{2g}	941	924 vw	26;27		…943	…927 w	15				
44	**D6**	B_{3u}	941 vs	920 vs	26;27				15				
45	**A3**	A_g	971	NA	32				18				
46	**C4**	A_u	977	NA	28;29	A_u;B_{1g}	978;	NA ;	16	A_2	978	NA ; 975 sh	**C-H ⊥bend… + Ph ⊥-twist**
47	**C4**	B_{1g}	978	NA	28;29		…978	…977 vw					
48	**C4**	A_u	978	NA	28;29								
49	**D7**	B_{2g}	999	NA	30;31	B_{3u};B_{2g}	1017 m;	966 m ;	17	B_1	1017 w	NA ; NA	**C-H ⊥bend… Ph -chair bend**
50	**D7**	B_{2g}	1016	962 vw	30;31		…1017	… NA	17				
51	**D7**	B_{3u}	1016 m	966 m	30;31				17				
52	**A3**	B_{1u}	1027 w	987 vw	32	A_g	1021	1002 vs	18	A_1	1036 w	1001 vw; 1003 vs	**Ph ‖-def. (breath)**
53	**A3**	B_{1u}	1049 s	999 w	33	B_{1u}	1050 m	999 m	18				
54	**A3**	A_g	1051	1002 s	33				18				
55	**B4**	B_{3g}	1098	1082 vw	35;36	B_{3g};B_{2u}	1098;	1083 m;	19	B_2	1098 vw	1070 s; 1070 m	**C-H ‖-bend**
56	**B4**	B_{2u}	1098 w	1070 vs	35;36		…1098 w	…1070 vs	19				
57	**A4**	B_{1u}	1108 w	1028 s	34	A_g	1095	1028 s	20	A_1	1114 vw	1026 s; 1032 s	**C-H ‖-bend… + Ph breath**
58	**B4**	B_{2u}	1123 w	1105 s	35;36				19				
59	**A4**	A_g	1128	1038 vw	37	B_{1u}	1142 vw	1026 s	20				
60	**A5**	B_{1u}	1149 m	1159 w	38	A_g	1149	1165 m	21	A_1	1149 vw	1153 w; 1168 vw	**C-H ‖-bend**
61	**A5**	A_g	1149	1133 vs	38				21				
62	**A5**	A_g	1150	1163 w	41	B_{1u}	1155 m	1157 m	21				
63	**B5**	B_{3g}	1152	NA	39;40	B_{3g};B_{2u}	1152;	1179 w;	22	B_2	1152 vw	1178 vw; 1185 w	**C-H ‖-bend**
64	**B5**	B_{2u}	1152 vw	1178 m	39;40		…1152 vw	…1178 w	22				
65	**B6**	B_{3g}	1209	NA	42;43	B_{2u};B_{3g}	1216 vw ;	1281 m;	23	B_2	1216 vw	1282 w; 1289 w	**C-H ‖-shear**
66	**B6**	B_{3g}	1216	1283 vw	42;43		…1216	…1281 m	23				
67	**B6**	B_{2u}	1216 vw	1281 s	42;43				23				
68	**A6**	B_{1u}	1240 m	1105 s	46	A_g	1313	1145 vs	25				
69	**B7**	B_{2u}	1308 w	1333 w	44;45	B_{3g} ;B_{2u}	1308;	1334 w;	24	B_2	1308 w	1331 vw; 1337 w	**Ph ‖-def.**
70	**B7**	B_{3g}	1308	1335 vw	44;45		…1308 w	…1331 m	24				
71	**B7**	B_{2u}	1317 w	1360 w	44;45				24				
72	**A6**	A_g	1334	1191 s	46				25	A_1	1361 w	NA; 1196 vs	**C-Ph str… + C-H ‖-shear**
73	**A6**	B_{1u}	1417 s	1311 m	47	B_{1u}	1447 s	1313 s	25				
74	**A6**	A_g	1510	1320 w	47				25				
75	**B8**	B_{2u}	1525 s	1406 s	48;49	B_{3g};B_{2u}	1536;	1444 m;	26	B_2	1536 s	1444 s; 1452 m	**C-H ‖-shear… + Ph ‖-def.**
76	**B8**	B_{2u}	1536 vs	1441 vs	48;49		…1536 vs	…1443 vs	26				
77	**B8**	B_{3g}	1536	1445 w	48;49				26				
78	**A7**	B_{1u}	1592 s	1483 s	50	A_g	1583	1484 s	27	A_1	1604 vs	1489 vs; 1495 s	**C-Ph str… + Ph ‖-def.**
79	**A7**	A_g	1658	1498 w	51	B_{1u}	1682 vs	1494 vs	27				
80	**A7**	B_{1u}	1711 vs	1516 vs	51				27				
81	**B9**	B_{3g}	1756	1548 vw	52;53	B_{3g};B_{2u}	1771;	1574 sh;	28	B_2	1772 vw	1574 w; 1579 sh	**Ph def. str.**
82	**B9**	B_{2u}	1771 w	1570 m	52;53		…1771 w	…1572 m	28				
83	**B9**	B_{3g}	1771	~1570	52;53				28				
84	**A8**	A_g	1793	1592 vs	54	A_g	1792	1591 vs	29	A_1	1796 w	1599 m; 1604 vs	**C-Ph str… + Ph ž-def.**
85	**A8**	B_{1u}	1803 vs	1595 vs	55	B_{1u}	1811 vs	1601 vs	29				
86	**A8**	A_g	1817	1603 m	55				29				
87	**A9**	A_g	2453	2214 vs	56	A_g	2456	2223 vs	30	A_1	2334 vs	2114 vs	**C≡C str.**
88	**A9**	B_{1u}	2455	2218 vw	56				30				

Table 3 (*Continued*)

89	**A10**	B_{1u}	3056 w	3020 m	57;58	$B_{1u};A_g$	3056w;	3020 m;	31	A_1	3056 w	3022 w;3028 vw	**C-H str.**
90	**A10**	A_g	3056	3024 w	57;58		…3056	…3023 vw	31				**(Ph def.)**
91	**B10**	B_{3g}	3059	3036 w	59;60	$B_{3g};B_{2u}$	3059;	3037 vw;	32	B_2	3059 vw	3033 w; NA	**C-H str.**
92	**B10**	B_{2u}	3059w	3032 m	59;60		…3059w	…3032 m	32				**(Ph def.)**
93	**B10**	B_{3g}	3059	3036 w	59;60				32				
94	**A11**	B_{1u}	3060 vs	3054 s	61;62	$B_{1u};A_g$	3067 vs;	3054 s;	33	A_1	3067 vs	3059 s; NA	**C-H str.**
95	**A11**	B_{1u}	3067 vs	3054 s	61;62		…3067	…3055 s	33				**(Ph def.)**
96	**A11**	A_g	3067	NA	61;62				33				
97	**B11**	B_{2u}	3072 vs	3060 sh	63;64	$B_{3g};B_{2u}$	3073;	3069 vs;	34	B_2	3073 vs	3064 sh;3067 vs	**C-H str.**
98	**B11**	B_{3g}	3073	3063 vs	63;64		…3073 vs	…3064 sh	34				**(Ph def.)**
99	**B11**	B_{2u}	3073 vs	3060 sh	63;64				34				
100	**A12**	A_g	3075	NA	65;66	$B_{1u};A_g$	3081 vs;	3078 m;	35	A_1	3082 vs	3080 s; NA	**C-H str.**
101	**A12**	B_{1u}	3081 vs	3078 m	65;66		…3082	…3084 sh	35				**(Ph breath)**
102	**A12**	A_g	3081	3084 w	65;66				35				

[a] For best clarity, each sub-group text-box, is filled by different gray shade. All information regarding a specific mode # assignment is described only once in the table: for empty cell see preceding cell with the same mode #. In the last column: ⊥ or ∥ refers to the molecular plane; indexes with superscripts: ž, etc. refers to the respective molecular symmetry axis. For example: 'Ph ⊥ bend' means, Ring bending perpendicular to the molecular plane. 'C–Ph ž-def.' means, C–Ph deformations in ž reference direction. Mode numbering scheme for each compound, is derived according to the energy calculated ascending order. Qualitative IR/Raman: 'vw', 'w', 'm', 's', 'vs' and 'sh', accounts for the respective: 'very weak', 'weak', 'medium', 'strong', 'very strong' and 'shoulder' intensities. Single asterisks denote data taken from [8]; double asterisks denote normal modes of PAs: #13 and #14 are the terminal hydrogen C–H bending modes. Mode: #36, is a terminal hydrogen C–H stretching mode, it has no relevancy to the DPA/DPB, therefore not shown in the table; triple asterisks denote a phenomenological mode assignment in the last column as described. Presumably, in this way, one can readily deduce the mode dynamics. However, in most conjugated molecular network this intuitive mode classification could easily mislead. Here, next to the formal mode type assignment, modes are specified phenomenologically.

respectively. D4 subgroup modes are out-of-plane C–Ph chair like bending vibrations. All the calculated frequencies are 5% lower then when measured. D5 and D6 subgroup's modes are out-of-plane C–H bending vibrations in $725 \div 765\ cm^{-1}$ region and at $918\ cm^{-1}$, respectively. In D5, IR and Raman active modes were almost degenerate. Due to a very strong IR absorption in all of three compounds and strong Raman scattering in the PA and the DPA the observed and calculated modes were readily correlated. In D6, IR absorption is very strong for the DPB and the DPA and strong for the PA. An additional, very strong IR vibration locates at $839\ cm^{-1}$ in the DPB. Raman modes of the D6 subgroup are less prominent but noticeable. The calculated and observed frequencies were easily correlated with 2.5% discrepancy.

B8 subgroup modes are in-plane phenyl-deformation, perpendicular to the principal symmetry axis vibrations, located at $1445\ cm^{-1}$. A strong mode in PA in IR is accompanied by a weak mode in Raman. In DPA and in DPB, a very strong IR active and a weak Raman active modes, positioned as a degenerate pair. One B_{2u} mode appears at $1406\ cm^{-1}$ in DPB. The calculated mode frequencies are 7% higher then the one measured.

A7 subgroup modes are phenyl-deformation along the symmetry axis vibrations, located at $\sim 1490\ cm^{-1}$. In PA, A_1 fundamental is strong in IR ($1489\ cm^{-1}$) and in Raman ($1495\ cm^{-1}$). In DPA, it splits in $1484\ cm^{-1}$ Raman (strong) and $1494\ cm^{-1}$ IR (very strong) active modes. In DPB, due to subsequent splitting, three modes, members in A7 subgroup are observed: $1483\ cm^{-1}$ (IR-strong), $1492\ cm^{-1}$ (Raman-medium) and $1516\ cm^{-1}$ (IR-very strong). A8 subgroup modes, are phenyl stretching along the symmetry axis vibrations, located at $\sim 1600\ cm^{-1}$. It has a similar to A7 unfolding scheme. A very strong IR (medium size Raman intensity) PAs A_1 mode is split into IR ($1601\ cm^{-1}$) and Raman ($1591\ cm^{-1}$) active modes in DPA following a threefold splitting in the DPB: $1592\ cm^{-1}$ (Raman), $1595\ cm^{-1}$ (IR) and $1603\ cm^{-1}$ (Raman). The difference between the

calculated and the measured frequencies are 11% for the A7 and A8 modes.

The remaining medium and weak intensity modes, which are observed in the spectra, were then assigned with some correlation to the locations of the closest ''anchor'' modes. The derived mode assignments are very close to those reported by Shimojima and Takahashi [7] for the DPA, PA (for some reason all the B_1 and B_2 modes were inverted) and by Attila et al. [6] for the PA. Minor discrepancies are found in assigning nearby modes of a similar intensity.[1] Some uncertainty arises in setting the modes in $920 \div 1080\ cm^{-1}$ region. Here, the four assigned sub-groups (A4, B4, A3 and D7) modes, are separated in some cases only by a few wavenumbers, and linear dichroic (polarized) IR (Raman) measurements are required to resolve a possible ambiguity. In previous studies [7], medium size IR mode at $966\ cm^{-1}$, was considered as A_u type of the C4 subgroup, while modes at $985\ cm^{-1}$ were identified as CH out-of-plane bending of the D7 subgroup symmetry. However, as it was pointed-out, IR vibrations of 'C' group are generally forbidden and since $966\ cm^{-1}$ IR vibration can not be constructed from any mode combination, it is assigned here to the B_{3u} type of the D7 subgroup. Modes in the $985\ cm^{-1}$ region are then interpreted as combinations.

The two CH in-plane bends of A5 and B5 subgroups are best correlated in all three compounds, when assigned near the 1162 and $1176\ cm^{-1}$, respectively, in opposite to the previous assignment [7]. The B6 subgroup assignment near $1280\ cm^{-1}$ is assisted by the nearby Fermi enhanced mode at $1267\ cm^{-1}$ of the 'B' subgroup origin. The A6 highly conjugated C-phenyl stretching although shifted by an average 9% from the calculated position has plausible features of a classic unfolding scheme.

In this study, the IR active CH stretching vibration assignments and their Raman counterpart in the $3000 \div 3100\ cm^{-1}$ region, are perfectly matched. However, some of the stretching mode assignments, are altered in this paper in respect to that of Shimojima and Takahashi [7] and Attila et al. [6], which are also distinct in respect to each other. After accounting for the PAs terminal hydrogen stretching ($3294\ cm^{-1}$), in-plane ($654\ cm^{-1}$) and out-of-plane ($621\ cm^{-1}$) bending vibrations, the fundamentals assignment is complete. Yet, several vibrations with weak or medium intensities are present.

A group of vibrations in the region: $1650 \div 1950\ cm^{-1}$, are assigned here to some IR active combinations, common in many molecules [23]. A proper overtones and combinations identification scheme may confirm the normal modes assignment, since both elements are ought to be members of a same sub-group: A, B, C or D. Number of medium-strong size Raman vibrations in the three compounds, were observed near a very strong $2200\ cm^{-1}$ C≡C stretching mode. Most of the possible overtones in this spectral region should originated from the elements of an 'A' group (see Table 3), which then were intensified due to Fermi resonance interaction with the A9 C≡C vibration.

To summarize, one can readily see, that modes, members mostly of the 'B', 'C' and 'D' symmetry groups, are effectively de-coupled, therefore displaying a simple manifold of almost degenerate in-phase and out-of-phase pattern. However, fundamentals originated in a parent's 'A'-symmetry group, are highly diverse. Since modes of 'A' symmetry group (B_{1u}, A_g), acts always along the principle symmetry axis, which is parallel to the acetylene C≡C bond, the interaction within the pair of the composing stretching mode elements for this symmetry type, is considerable as may be expected. Yet, our main presumption, as, to the vibronic de-coupling of the seemingly conjugated pair of the parent DPA (and correspondingly, the de-coupling of the PA mode pair in the DPA), was justified in general.

4.4. Overtones and combinations in the 500 ÷ 1600 cm^{-1} region

For the members of the D_{2h} point group, the first overtone is always IR forbidden and Raman allowed, while some of the combinations are IR or Raman allowed (but not both). Only members of a same symmetry sub-group can form an optically active combination. Combinations of modes subscripted

[1] For example, modes #6 (B_1) and #7 (B_2) (Table 3) of the PA assigned at 515 (medium) and 530 (strong) (cm^{-1}), were inverted in [6,7]. The A5 and B5 sub-group modes, which are only $15\ cm^{-1}$ apart from each other, were inverted according to the assignment in this work. Assignment of DPA Raman modes at 710 (strong) and 691 (medium) (cm^{-1}), is opposite in respect to that of [7].

Table 4
IR and Raman active overtones and combinations

PA		DPA		DPB	
Found in...	Originated from...	Found in...	Originated from...	Found in...	Originated from...
IR active overtones and combinations					
1115w	B_1 (762vs) + B_1(361vs)	[a]667m	B_{3u} (280s) + B_{2g} (388s)	877vw	B_{3u} (550s) + B_{2g} (334m)
1240w	[b]$2B_1$ (622vs)	791vw	A_g (261s) + B_{1u} (536s)	984vw	B_{3u} (523vs) + B_{2g} (470m)
1300sh	[b]$2B_2$ (653vs)	823w	B_{3u} (280s) + B_{2g} (543s)	1021s	B_{3u} (550s) + B_{2g} (470m)
1383m	$2B_1$ (690vs)	[a]894w	B_{2g} (388s) + B_{3u} (509vs)	1021s	B_{2g} (334m) + B_{3u} (692vs)
1457w	B_1 (762vs) + B_1 (690 vs)	[a]985m	B_{3u} (280s) + B_{2g} (710s)	1217vw	B_{3u} (754vs) + B_{2g} (470m)
1472vw	A_1 (1003vs) + A_1 (474vs)	[a]1103m	B_{3g} (626s) + B_{2u} (467m)	[a]1267m	B_{3g} (654w) + B_{2u} (623w)
		1219vw	B_{3u} (509vs) + B_{2g} (710s)	1306sh	B_{3u} (839vs) + B_{2g} (470m)
		1227vw	B_{1u} (536s) + A_g (691m)	1386m	B_{2g} (470m) + B_{3u} (920vs)
		1229vw	B_{3u} (690vs) + B_{2g} (543s)	1450w	B_{2g} (537m) + B_{3u} (920vs)
		1244vw	B_{3u} (280s) + B_{2g} (966m)	1539w	B_{3g} (477m) + B_{2u} (1070vs)
		1388m	B_{3u} (690vs) + B_{2g} (710s)		
		1536m	A_g (1002vs) + B_{1u} (536s)		
Raman active overtones and combinations					
1034m	B_1 (690vs) + B_1 (349s)	1084m	$2B_{2g}$ (543s)	864vw	B_{2g} (334m) + B_{2g} (537m)
1236w	[b]$2B_1$ (622vs)	1192w	B_{3u} (280s) + B_{3u} (918vs)	1038vw	$2B_{3u}$ (523vs)
1380w	$2B_1$ (690vs)	1313vw	B_{2g} (388s) + B_{2g} (927w)	[a]1104w	$2A_g$ (554w)
		1380vw	$2B_{3u}$ (690vs)	1379w	$2B_{3u}$ (692vs)
		1538w	B_{2u} (470m) + B_{2u} (1070vs)		

[a] Fermi resonance induced combination (overtone).
[b] CH bending of terminal hydrogen in PA. Not shown in Table 3. Intensity indexes are as in Table 3.

identically: 'g × g' or 'u × u' are Raman active. Combinations are expected to be IR active when both elements subscripted differently: 'g × u'. For the C_{2v} point group, overtones and combinations, members of a same sub-group, are IR and Raman allowed. Combinations, members of the 'C' group are IR inactive.

The proposed overtones and combinations pattern is given in Table 4. The suggested scheme facilitates setting of several Raman/IR active modes at their exact position. For example: Raman active A1 and D3 nearby fundamentals in the DPB, positioned at 537 and 554 cm^{-1}, respectively, although the inverse assignment is acceptable as well. However, only when chosen correctly, the observed weak combination at 1450 cm^{-1} can be explained. The same basic argumentation, when applied to a medium sized combination at 1388 cm^{-1}, guided us, as to establishing the correct ordering of D4 and A2 Raman modes in the DPA. Some possible combinations detected in the DPB as a very weak IR modes at 720 or 740 cm^{-1}, were left unassigned, since we were not able to measure the IR spectra bellow 450 cm^{-1}. After careful examination (and in few numbered cases, reordering of the nearby modes), all the observed combinations and overtones were assigned. Certain weak or even medium sized non-fundamentals are considered as Fermi resonances, due to a plausible existence of symmetry related nearby fundamentals.

5. Conclusions

The vibrational spectra of the PA, DPA, DPB molecules, acquired by Raman and IR techniques, were analyzed by means of a computationally efficient semiempirical PM3 method, in a framework of inclusive correspondence. Fundamentals, overtones and combinations for the three compounds were identified. Here, the assumption was tested, as to whether the vibrational spectra of a series of symmetry related molecules, building together a chain of ascending complexity, could be correlatively examined in order to predict the vibrational spectrum for the next multiple element (DPB as a test case in the present study). This was made possible, due to the vibronic

de-coupling within the composing modes of the ''building'' elements. The degenerate nature of the composed fundamentals, prevailed in modes with components, perpendicular to the principal axis symmetry. Modes of symmetry: B_{1u}, A_g, with major components parallel to the acetylene C≡C bond, where split. It is concluded, that for a more complex molecular chain (DPB + PA . . .), but still confined to the D_{2h} point group (LPAS), the present analysis could be further utilized. However, if a similar correlation analysis for a lower symmetry PAMC would exercised, it is implied, that interactions among the adjacent symmetry members, with directional elements perpendicular to the principal LPAS axis (but parallel to some acetylene elements of the PAMC), would obstruct any straightforward mode interpretation, as presented here.

Acknowledgements

We would like to thank Dr. A. Tishbee from the Weizmann Institute of Science, for enabling us to use the Raman spectrometer. We would like to thank Prof. V. Khodorkovsky from the Ben-Gurion University, for enabling us to use the HyperChem 5.0 software.

References

[1] Z. Jinsan, S.M. Jeffrey, X. Zhifu, A.A. Ryan, J. Am. Chem. Soc. 114 (1992) 2273.
[2] Z. Jinsan, J.P. Douglas, L.L. James, S.M. Jeffrey, J. Am. Chem. Soc. 116 (1994) 4227.
[3] J. Zang, J.S. Moore, J. Am. Chem. Soc. 114 (1992) 9701.
[4] I. Pri-Bar, J.E. Koresh, J. Mol. Catal. A 156 (2000) 173.
[5] A. Dhiranie, R.W. Zehner, R.P. Hsung, P. Guyot-Sionnest, R.L. Sita, J. Am. Chem. Soc. 118 (1996) 3319.
[6] G.C. Attila, F. Geza, E.B. James, J. Phys. Chem. 93 (1989) 7644.
[7] A. Shimojima, H. Takahashi, J. Phys. Chem. 97 (1993) 9103.
[8] P. Alcolea, Spectrosc. Lett. 29 (2) (1996) 241.
[9] W. Meyer, P. Pulay, Theor. Chim. Acta 32 (1976) 253.
[10] P. Botschwina, Chem. Phys. Lett. 29 (1974) 98.
[11] P. Botschwina, Chem. Phys. Lett. 29 (1974) 580.
[12] C.E. Blom, C. Altona, Mol. Phys. 31 (1976) 1377.
[13] C.E. Blom, C. Altona, Mol. Phys. 32 (1976) 1137.
[14] C.E. Blom, C. Altona, Mol. Phys. 33 (1977) 875.
[15] C.E. Blom, C. Altona, Mol. Phys. 34 (1977) 177.
[16] D.M. Seeger, C. Korzeniewski, W. Kowalchyk, J. Phys. Chem. 95 (1991) 6871.
[17] P. Pulay, F. Geza, P. Gabor, E.B. James, A. Vargha, J. Am. Chem. Soc. 105 (1983) 7037.
[18] S. Harens, C.C. Yu, D. Daraney, C.S. Marvel, J. Polym. Sci. 19 (1981) 1349.
[19] M.J.S. Dewar, E.G. Zoebisch, E.F. Healy, J.J.P. Stewart, J. Am. Chem. Soc. 107 (1985) 3902.
[20] J.J.P. Stewart, J. Comput. Chem. 10 (1989) 209.
[21] H. Zuilhof, G. Lodder, J. Phys. Chem. 96 (17) (1992) 6957.
[22] G. Herzberg II. Infrared and Raman Spectra of Polyatomic Molecules, in: Molecular Spectra and Molecular Structure, 13th Edition, Van Nostrand Company, NJ, 1968, p. 237.
[23] J.B. Lambert, H.F. Shurvell, D.A. Lightner, R.G. Cooks, Organic Structural Spectroscopy, Prentice-Hall, NJ, 1998 (Chapter 9).